PERGAMON

International Journal of Solids and Structures 38 (2001) 445–455

INTERNATIONAL JOURNAL OF SOLIDS and STRUCTURES

www.elsevier.com/locate/ijsolstr

Analytical solution for compression stiffness of bonded rectangular layers

C.G. Koh *, H.L. Lim

Department of Civil Engineering, National University of Singapore, 10 Kent Ridge Crescent, Singapore 119260, Singapore

Received 15 November 1999; in revised form 24 February 2000

Abstract

It is well known that the compression stiffness of bonded layers increases due to the restricted lateral expansion if Poisson's ratio is near 0.5. While analytical solutions have previously been obtained for circular, infinite-strip and square shapes, this paper presents the first analytical attempt for bonded rectangular layers. On the basis of two kinematic assumptions and by means of variable transformation, the governing equations are derived. The double series approach provides a direct means of computation with second-order convergence. The solutions agree well with the published results for special cases of square layers and infinite strips, and with finite element results for rectangular layers. Besides illustrating the importance of including the compressibility effect, the numerical study shows that the effect of length-to-width ratio is significant on the effective compression modulus of rectangular pads.

Keywords: Compression modulus; Rubber; Compressibility; Rectangular layer; Series solution

1. Introduction

Elastomeric pads and bearings are commonly used for the purpose of vibration isolation. Usually made of natural or synthetic rubbers, they could be used at the vibration "source" such as machineries to reduce the vibrations transmitted to the supporting structures. Alternatively, they could be installed at the "target" e.g. to protect sensitive instruments in a noisy factory environment using thin elastomeric pads. For the same reason, it is possible to use rubber bearings at the base of buildings and structures alike to reduce traffic-induced vibration. The first building to be isolated from low frequency ground-borne traffic vibration by means of natural rubber bearings was an apartment built in London in 1966 (Kelly, 1997). In recent years, the concept of using base isolation bearings for earthquake resistant design of buildings and bridges has been increasingly accepted. The aim is to reduce the forces transmitted to the structures in the event of earthquakes. Such bearings typically consist of several thin rubber layers sandwiched between and bonded to steel reinforcing plates.

* Corresponding author.

0020-7683/00/$ - see front matter
PII: S0020-7683(00)00057-3

Under vertical compression, the expansion of bonded rubber layers is confined in only lateral directions. As rubber is highly incompressible (Poisson's ratio v close to 0.5), the restricted expansion results in higher compression modulus than in the case of unbonded rubber layers. The effective compression modulus can be defined as

$$E_c = \frac{P}{A\varepsilon_t}, \tag{1}$$

where A is the area of the pad, t the thickness, and ε_t the average thickness strain (or relative change in thickness) under a compression load P. The value of E_c is larger than Young's modulus (E) of the material by even one or two orders of magnitude, depending upon the shape factor and Poisson's ratio. The shape factor is defined as the ratio of the loaded area to the stress-free area (where lateral expansion takes place). Earlier works assumed strict incompressibility, i.e. v is exactly equal to 0.5. On this basis, Gent and Lindley (1959) derived the effective compression modulus for pads of two types of geometry, i.e. circular pads and infinitely long pads. In addition, the following assumptions were made (two on kinematics and one on stress):

(A) horizontal plane sections remain plane,

(B) vertical lines become parabolic after deformation under compression loading (parabolic "bulging" shape),

(C) normal stress components in all the three orthogonal directions are the same and equal to the mean pressure.

This approximate treatment was further extended by Lindley (1966) and Gent and Meinecke (1970) to pads of other shapes including ellipse, square, rectangle and equilateral triangle. Nevertheless, for pads of high shape factor, the assumption of strict incompressibility for material overestimates the effective compression modulus considerably. This is not desirable as it leads to the over-estimation of the buckling load and resonant frequency. Even though the numerical value of Poisson's ratio may be very close to 0.5, the effect of material compressibility cannot be neglected. In an energy approach, Lindley (1979) derived the compression moduli for elastic blocks bonded to rigid end plates for plane strain (infinitely long strip) and axisymmetric (circular) cases. In addition to assumptions (A) and (B) mentioned above, two assumptions were made regarding the magnitudes of normal strains and the bulk strain. This approach was found to be applicable for materials with Poisson's ratio between 0.125 and 0.49983 and the width-to-thickness ratio between 0.25 and 128. In a similar investigation, Moghe and Neff (1971) derived the effective compression modulus for constrained elastic cylinders in terms of infinite series of orthogonal Bessel and trigonometric functions.

Accounting for the effect of compressibility, Chalhoub and Kelly (1990) formulated a theoretical approach to derive the compression stiffness of circular layers used in rubber isolation bearings. Based on assumptions (A)–(C), the governing equations for the "hydrostatic pressure" in a bonded rubber layer were presented. Known as the "pressure" solution, the approach was extended to treat infinite strips (Chalhoub and Kelly, 1991), hollow circular pads (Constantinou et al., 1992) and square pads (Kelly, 1997).

In the pressure solution approach, it is necessary to assume that the state of stress at any point in the material behaves like fluid, and hence the governing equation can be expressed in terms of the hydrostatic pressure term. This is a rather ad hoc assumption. Without making this assumption, Koh and Kelly (1989) proposed two direct solutions to compute the effective compression modulus of bonded *square* elastomeric layers. The first direct solution is based on the two kinematic assumptions (A) and (B). It is noteworthy that the solution method takes advantage of the so-called square symmetry (about diagonals). This solution is almost indistinguishable numerically from the second direct solution that further eliminates kinematic assumption (B), thereby confirming that the assumption of parabolic bulging shape is a realistic one. The error due to the remaining assumption (A) is also shown to be negligible for typical shape factors. Both direct solutions recover the effective compression modulus to Young's modulus when Poisson's ratio

approaches zero. In contrast, the pressure solution fails to do so and is thus applicable to only a limited range of Poisson's ratio. In a similar attempt without assuming fluid-like stress state, Tsai and Lee (1998) recently obtained closed form solutions for bonded layers of infinite-strip, circular and square shapes. For square layers, square symmetry is made use of as in the solution presented by Koh and Kelly (1989). The solution also involves an infinite series, though in a more complicated form requiring the solution of a matrix equation. The rapid convergence of the series solution gives good accuracy with the use of only one term. The numerical results compare well with the results given by Koh and Kelly (1989).

Rectangular pads are not uncommon for isolation support of machines and railway tracks. Nevertheless, no analytical solution thus far has been presented taking into account the effect of compressibility. This is in fact the main reason why solutions have been obtained for infinite-strip layers as an approximation for long rectangular layers. In this paper, the approach similar to the first direct solution of Koh and Kelly (1989) is adopted, but without the benefit of square symmetry.

2. Theoretical formulation

Consider a rectangular layer bonded between two rigid plates and subjected to a vertical compression load, P. The layer is of thickness t, width $2a$ and length $2b$. The material is assumed to be linearly elastic, homogenous and isotropic. A Cartesian coordinate system (x_1, x_2, x_3) is established with the origin at the center of the mid-plane as shown in Fig. 1.

Let u_i denote the displacement component in the x_i direction. The top and bottom surfaces of the layer are perfectly bonded to rigid plates so that $u_1 = u_2 = 0$ at $x_3 = \pm t/2$. Following the usual definition, the shape factor for a bonded rectangular layer is

$$S = \frac{ab}{t(a+b)}. \tag{2}$$

Kinematic assumptions (A) and (B), which are found to be reasonable in the study for square layers (Koh and Kelly 1989), are adopted here. Accordingly, the displacements can be expressed as follows:

$$u_i(x_1, x_2, x_3) = \bar{u}_i(x_1, x_2)(1 - 4x_3^2/t^2) \quad \text{for } i = 1, 2, \tag{3}$$

$$u_3(x_1, x_2, x_3) = \bar{u}_3(x_3). \tag{4}$$

Using the usual tensor notations for stress (σ_{ij}) and strain (ε_{ij}), the constitutive equation and strain–displacement relation are, respectively,

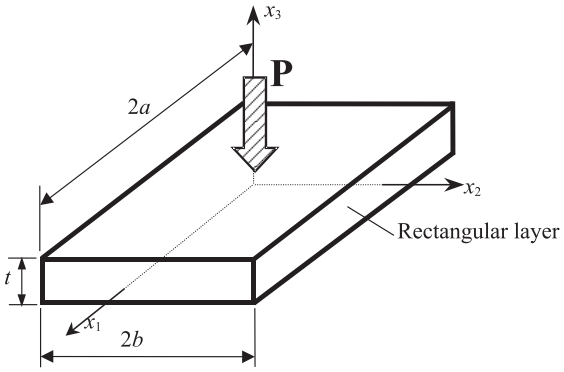

Fig. 1. Geometry and co-ordinate system for a rectangular layer bonded between two rigid plates.

$$\sigma_{ij} = \lambda\varepsilon_{kk}\delta_{ij} + 2\mu\varepsilon_{ij}, \tag{5}$$

$$\varepsilon_{ij} = \tfrac{1}{2}(u_{i,j} + u_{j,i}), \tag{6}$$

where δ_{ij} is the Kronecker delta function, μ is the same as the shear modulus G, and $\lambda = vE/[(1+v)\times(1-2v)]$. It can be shown that

$$\sigma_{11} = \left[(\lambda+2G)\bar{u}_{1,1} + \lambda\bar{u}_{2,2}\right]\left(1-4x_3^2/t^2\right) + \lambda\bar{u}_{3,3}, \tag{7}$$

$$\sigma_{22} = \left[(\lambda+2G)\bar{u}_{2,2} + \lambda\bar{u}_{1,1}\right]\left(1-4x_3^2/t^2\right) + \lambda\bar{u}_{3,3}, \tag{8}$$

$$\sigma_{33} = (\lambda+2G)\bar{u}_{3,3} + \lambda\left(\bar{u}_{1,1} + \bar{u}_{2,2}\right)\left(1-4x_3^2/t^2\right), \tag{9}$$

$$\sigma_{13} = \sigma_{31} = -8G\bar{u}_1 x_3/t^2, \tag{10}$$

$$\sigma_{23} = \sigma_{32} = -8G\bar{u}_2 x_3/t^2, \tag{11}$$

$$\sigma_{12} = G\left(\bar{u}_{1,2} + \bar{u}_{2,1}\right)\left(1-4x_3^2/t^2\right). \tag{12}$$

The compression load P is obtained by integrating σ_{33} over the mid-plane, leading to

$$P = -(\lambda+2G)A\bar{u}_{3,3} - \lambda\left(1-4\frac{x_3^2}{t^2}\right)\int_A(\bar{u}_{1,1}+\bar{u}_{2,2})\mathrm{d}A. \tag{13}$$

Integrating the above equation over the thickness and substituting the result into Eq. (1) results in

$$E_c = (\lambda+2G)\left[1 - \frac{2}{3}\frac{\bar{\lambda}}{A\varepsilon_t}\int_A(\bar{u}_{1,1}+\bar{u}_{2,2})\mathrm{d}A\right], \tag{14}$$

where $\bar{\lambda} = \lambda/(\lambda+2G) = v/(1-v)$. To evaluate $u_{1,1}$ and $u_{2,2}$ as required above, the following equilibrium equation is invoked:

$$\sigma_{ij,j} = 0. \tag{15}$$

Substituting Eqs. (10) and (12) into the above equation with $i=1$, differentiating the resulting equation with respect to x_1 and finally integrating through the thickness leads to

$$\sigma_{11,11} = \frac{8G\bar{u}_{1,1}}{t^2} - \frac{2}{3}G(\bar{u}_{1,122} + \bar{u}_{2,211}). \tag{16}$$

An alternative expression can be obtained by differentiating Eq. (7) twice with respect to x_1 and integrating through the thickness

$$\sigma_{11,11} = \frac{2}{3}\left[(\lambda+2G)\bar{u}_{1,111} + \lambda\bar{u}_{2,211}\right]. \tag{17}$$

Equating the above two expressions and dividing by $(\lambda+2G)$ gives

$$12\bar{G}\bar{u}_{1,1}/t^2 = \bar{u}_{1,111} + (\bar{\lambda}+\bar{G})\bar{u}_{2,211} + \bar{G}\bar{u}_{1,122}, \tag{18}$$

where $\bar{G} = G/(\lambda+2G) = (1-2v)/2/(1-v)$. Similarly, for $i=2$ in Eq. (15),

$$12\bar{G}\bar{u}_{2,2}/t^2 = \bar{u}_{2,222} + (\bar{\lambda}+\bar{G})\bar{u}_{1,122} + \bar{G}\bar{u}_{2,211}. \tag{19}$$

Eqs. (18) and (19) provide the governing equations for solving $\bar{u}_{1,1}$ and $\bar{u}_{2,2}$. The corresponding boundary conditions are derived by imposing stress-free condition along the four lateral sides:

$$\sigma_{11}\ (x_1 = \pm a, x_2) = 0 \tag{20}$$

$$\sigma_{22}\ (x_1, x_2 = \pm b) = 0. \tag{21}$$

Substituting Eqs. (7) and (8) into Eqs. (20) and (21), respectively, and integrating both resulting equations through the thickness results in

$$\bar{u}_{1,1} + \bar{\lambda}\bar{u}_{2,2} = \tfrac{3}{2}\bar{\lambda}\varepsilon_t \quad \text{at } x_1 = \pm a, \tag{22}$$

$$\bar{u}_{2,2} + \bar{\lambda}\bar{u}_{1,1} = \tfrac{3}{2}\bar{\lambda}\varepsilon_t \quad \text{at } x_2 = \pm b. \tag{23}$$

The above boundary conditions can be made simpler by using the following "QR-transformation" (Koh and Kelly, 1989):

$$Q(x_1, x_2) = \bar{u}_{1,1}(x_1, x_2) + \overline{\lambda}\bar{u}_{2,2}(x_1, x_2) - \tfrac{3}{2}\bar{\lambda}\varepsilon_t, \tag{24}$$

$$R(x_1, x_2) = \bar{u}_{2,2}(x_1, x_2) + \bar{\lambda}\bar{u}_{1,1}(x_1, x_2) - \tfrac{3}{2}\bar{\lambda}\varepsilon_t. \tag{25}$$

Hence,

$$Q(x_1 = \pm a, x_2) = 0, \tag{26}$$

$$R(x_1, x_2 = \pm b) = 0. \tag{27}$$

Solving simultaneously Eqs. (24) and (25) gives the inverse transformation:

$$\bar{u}_{1,1} = \frac{Q - \bar{\lambda}R}{1 - \bar{\lambda}^2} + \frac{3}{2}\frac{\bar{\lambda}}{1 + \bar{\lambda}}\varepsilon_t, \tag{28}$$

$$\bar{u}_{2,2} = \frac{R - \bar{\lambda}Q}{1 - \bar{\lambda}^2} + \frac{3}{2}\frac{\bar{\lambda}}{1 + \bar{\lambda}}\varepsilon_t. \tag{29}$$

Eqs. (18) and (19) thus become

$$ab\Big(c_3 Q_{,11} + \bar{G}Q_{,22} + \bar{G}R_{,11} - \bar{\lambda}\bar{G}R_{,22}\Big) = c_1(Q - \bar{\lambda}R) + c_2\varepsilon_t, \tag{30}$$

$$ab\Big(c_3 R_{,22} + \bar{G}R_{,11} + \bar{G}Q_{22} - \bar{\lambda}\bar{G}Q_{,11}\Big) = c_1(R - \bar{\lambda}Q) + c_2\varepsilon_t, \tag{31}$$

where $c_1 = 12\bar{G}(ab/t^2)$, $c_2 = (3/2)c_1\bar{\lambda}(1 - \bar{\lambda})$ and $c_3 = 1 - \bar{\lambda}(\bar{\lambda} + \bar{G})$.

3. Series solution

As shown for square layers (Koh and Kelly, 1989; Tsai and Lee, 1998), the series approach provides a closed form solution to the problem and its rapid numerical convergence is an advantage. Square symmetry, e.g. $\bar{u}_1(x_1, x_2) = \bar{u}_2(x_2, x_1)$, is not valid here for rectangular layers. Thus, it is necessary to use double Fourier series instead of a single series.

By virtue of symmetry about the x_1 and x_2 axes, it follows that $\bar{u}_{1,1}$ and $\bar{u}_{2,2}$ are symmetric functions of both x_1 and x_2. Hence, only cosine functions are needed in the double series expressions for Q and R, as follows:

$$Q(x_1,x_2)=\sum_{m=1}^{\infty}\sum_{n=1}^{\infty}q_{mn}\cos(\alpha_m x_1/a)\cos(\beta_n x_2/b), \tag{32}$$

$$R(x_1,x_2)=\sum_{m=1}^{\infty}\sum_{n=1}^{\infty}r_{mn}\cos(\alpha_m x_1/a)\cos(\beta_n x_2/b), \tag{33}$$

where $\alpha_m=(m-0.5)\pi$ and $\beta_n=(n-0.5)\pi$. Eqs. (26) and (27), which result from imposing the boundary conditions as given in Eqs. (20) and (21), are satisfied by the above construction. Note that Eq. (32) also means $Q(x_1,x_2=\pm b)=0$. Nevertheless, this does not necessarily imply that $\sigma_{11}(x_1,x_2=\pm b)=0$ since the construction of Q from Eq. (20) involves integration through the thickness. An analogy is that $f(x)=0\Rightarrow\int f(x)\,\mathrm{d}x=0$, but the converse may not be necessarily true. In the context of the present formulation and assumptions, the only implication is that the integral of σ_{11} at $x_2=\pm b$ through the thickness is zero; similarly for σ_{22} at $x_1=\pm a$.

The coefficients q_{mn} and r_{mn} are derived by (i) differentiating the above two equations twice with respect to x_1 and x_2, (ii) substituting into Eqs. (30) and (31), and (iii) applying the orthogonality properties of cosine functions. After some simplification, the following expressions are obtained:

$$A_{mn}q_{mn}+B_{mn}r_{mn}=E_{mn}, \tag{34}$$

$$C_{mn}r_{mn}+D_{mn}q_{mn}=E_{mn}, \tag{35}$$

where

$$A_{mn}=-c_3\alpha_m^2\Omega-\bar{G}\beta_n^2\Omega^{-1}-c_1,\quad B_{mn}=-\bar{G}\alpha_m^2\Omega+\bar{\lambda}\bar{G}\beta_n^2\Omega^{-1}+c_1\bar{\lambda},$$
$$C_{mn}=-c_3\beta_n^2\Omega^{-1}-\bar{G}\alpha_m^2\Omega-c_1,\quad D_{mn}=-\bar{G}\beta_n^2\Omega^{-1}+\bar{\lambda}\bar{G}\alpha_m^2\Omega+c_1\bar{\lambda},$$
$$E_{mn}=\frac{4(-1)^{m+n}c_2\varepsilon_t}{\alpha_m\beta_n}$$

and $\Omega=b/a$ is the ratio of length to width, herein called the *aspect ratio*.

Solving the above two equations yields the expressions for q_{mn} and r_{mn}. These are then substituted into Eqs. (28) and (29) to obtain $\bar{u}_{1,1}$ and $\bar{u}_{2,2}$, and subsequently into Eq. (14). After much manipulation, the effective compression modulus can be expressed as

$$E_c=E+E\frac{96v^2}{1-v^2}\frac{ab}{t^2}\sum_{m=1}^{\infty}\sum_{n=1}^{\infty}\left[1+\frac{t^2}{12ab}\left(\alpha_m^2\Omega+\beta_n^2\Omega^{-1}\right)\right]\frac{1}{\alpha_m^2\beta_n^2F_{mn}}, \tag{36}$$

where

$$F_{mn}=\frac{t^2}{6ab}\left[2\alpha_m^2\beta_n^2+(1-v)\left(\alpha_m^4\Omega^2+\beta_n^4\Omega^{-2}\right)\right]+\frac{12ab}{t^2}\frac{1-2v}{1-v}+\frac{3-4v}{1-v}\left(\alpha_m^2\Omega+\beta_n^2\Omega^{-1}\right).$$

When $v=0$, the second term in Eq. (36) vanishes and the solution recovers correctly to Young's modulus. The above solution involves no trigonometric function, hyperbolic function or any special function (e.g. Bessel function) as encountered in most other solutions for this type of problem. The series approach can be easily implemented in a computer program or spreadsheet. The term ab/t^2 appears in several places in the above equation and may be a more natural term than the usual definition of shape factor S to measure the extent of constraint in lateral expansion. This term can be expressed in terms of the two geometric parameters S and Ω, noting that $a/t=S(1+\Omega^{-1})$ and $b/t=S(1+\Omega)$. Note also that the solution for a particular value of Ω is the same as that for $1/\Omega$ (irrespective of whether b is the longer or shorter side).

4. Numerical results and discussion

In order to (partially) verify the proposed method, three special cases are considered: a square layer, an elongated layer which may be idealized as an infinite strip, and a rectangular layer of aspect ratio equal to 2. In each case, two shape factors are studied: $S = 5$ and 20. For the proposed method, the series solution is computed for terms up to $m = n = 10$ (more than sufficient for the series convergence). The effective compression modulus is sensitive to the value of Poisson's ratio when the value is near 0.5. As adopted in previous works (Koh and Kelly, 1989; Tsai and Lee, 1998), the term $\log(1/(1-2v))$, rather than v itself, is a better measure of the "closeness" to strict incompressibility. Thus, the effective compression modulus (normalized with Young's modulus) is plotted versus this term.

4.1. Square layer

The present solution is obtained for $\Omega = 1$ and compared with the square-layer solution by Koh and Kelly (1989). As shown in Fig. 2, the present solution virtually coincides with the Koh–Kelly solution.

4.2. Elongated layer

The present solution is obtained for a very large aspect ratio of $\Omega = 50$ or, conversely, a very small value of 0.02. This is compared with the solution for the idealized infinite-strip (Tsai and Lee, 1998). Again, the agreement is found to be very good as shown in Fig. 3.

4.3. Rectangular layer of aspect ratio 2:1

A rectangular layer of $\Omega = 2$ (or 0.5) is considered. Since no closed form solution is available, numerical results are obtained by means of the finite element method using a software called SAP2000 (SAP2000, 1997). The layer is modelled as three sub-layers, each having 30 eight-node solid elements with incompatible bending modes. The finite element solution for the effective compression modulus is slightly larger than the

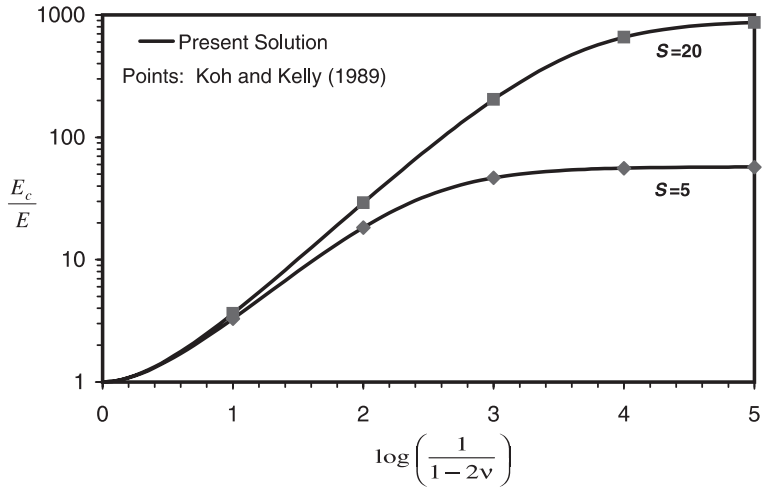

Fig. 2. Effective compression modulus for square layer ($b/a = 1$).

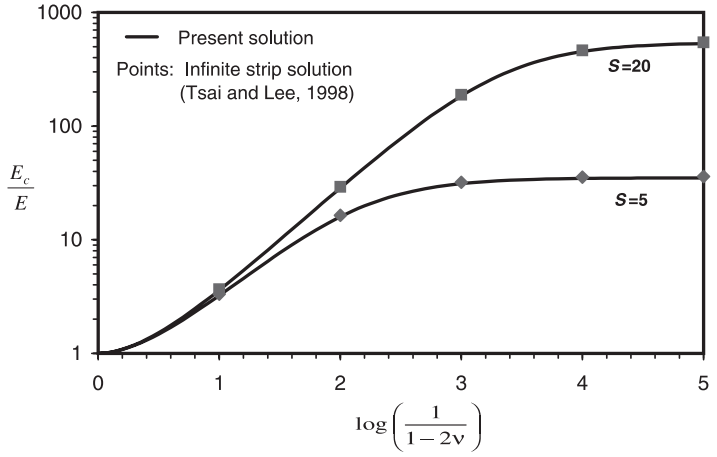

Fig. 3. Effective compression modulus for rectangular layer with $b/a = 50$ (or 0.02).

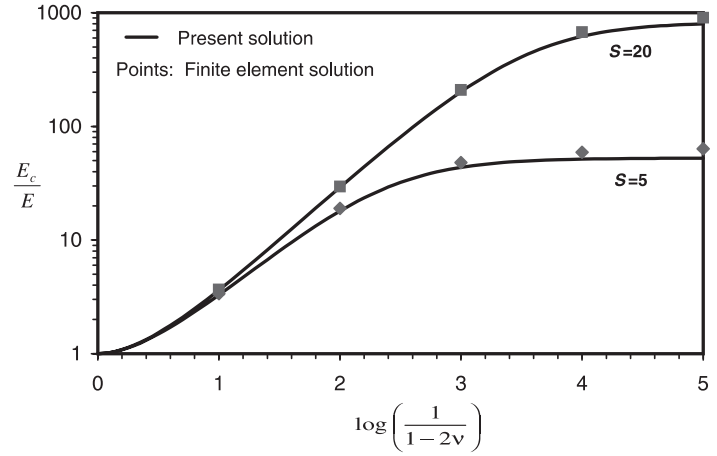

Fig. 4. Effective compression modulus for rectangular layer with $b/a = 2$ (or 0.5).

present solution (Fig. 4). This is not unexpected, as the finite element method tends to overestimate the stiffness in general.

4.4. Effects of aspect ratio

The present method is used to study the effects of aspect ratio. Let E_c^{SQ} denote the effective compression modulus for a square layer. The ratio of the effective compression modulus of the rectangular layer to E_c^{SQ} is presented for the full range of Ω (from nearly zero to one) in Figs. 5 and 6 for $S = 5$ and 20, respectively. The effective compression modulus for a rectangular layer ($\Omega \neq 1$) is always smaller than that for a square layer with the same shape factor. The reduction in E_c is significant for Poisson's ratio larger than 0.49 and can be as high as about 40% for v near 0.5.

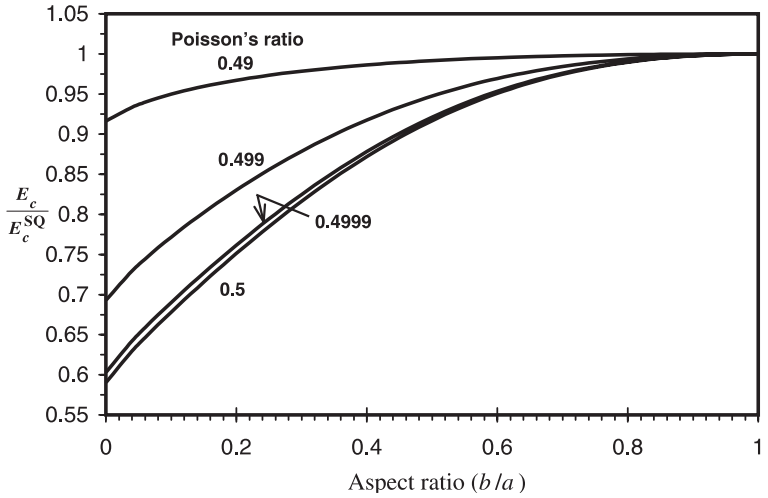

Fig. 5. Ratio of effective compression moduli for rectangular layer and square layer, for $S = 5$.

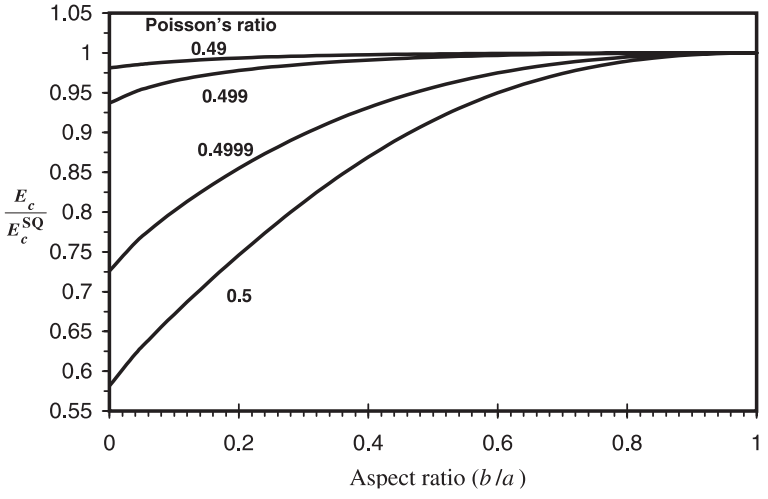

Fig. 6. Ratio of effective compression moduli for rectangular layer and square layer, for $S = 20$.

4.5. Convergence of series solution

Finally, the convergence of the series solution is studied. Let $E_c^{(m,n)}$ denote the solution computed using up to (m, n) terms. As the effect of aspect ratio is significant when Poisson's ratio is near 0.5, two such values are considered: $v = 0.49$ and 0.4999. As for the aspect ratio, $\Omega = 2$ and 20 are considered. The ratio of $E_c^{(1,1)}$ (i.e. using only the first term of the series) to $E_c^{(10,10)}$ (taken as the converged solution) is plotted in Fig. 7(a) for a very wide range of shape factor from 0.1 to 100. It is seen that the ratio $E_c^{(1,1)}/E_c^{(10,10)}$ may drop to 0.7, when the shape factor is very large. The practical values of shape factor are normally between 1 and 10. For this range, the error incurred by using only the first term of the series may be up to 20%.

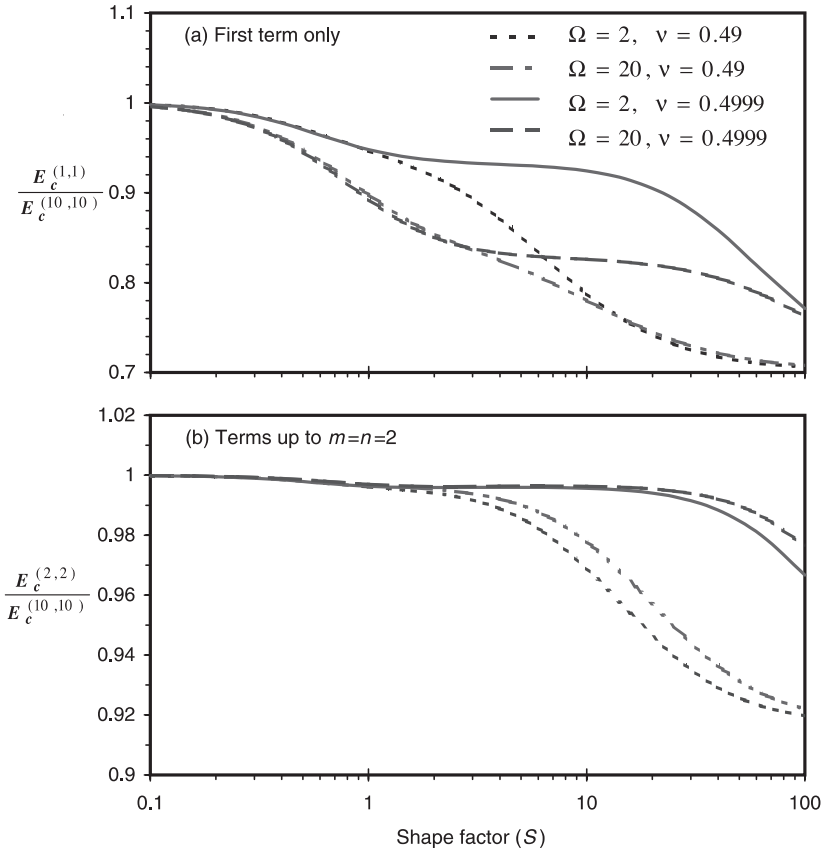

Fig. 7. Convergence of double series solution for rectangular layers.

The series solution computed using terms up to $m = n = 2$, i.e. $E_c^{(2,2)}$, is very close to the converged solution as illustrated in Fig. 7(b). The error incurred is up to about 5% for shape factors between 1 and 10. For v near 0.5, the single series solution for square layers (Koh and Kelly, 1989; Tsai and Lee, 1998) has roughly fourth-order convergence and thus the first term alone gives a very accurate solution. In the double series solution, which is needed here for rectangular layers, the (off-diagonal) term of $m = 2$ and $n = 1$ is of second order as compared to the first term of $m = n = 1$; similarly for the term of $n = 2$ and $m = 1$. Hence, it is generally necessary to include the first three terms that contain $m = 1$ and/or $n = 1$.

5. Conclusions

On the assumptions that horizontal plane sections remain plane and vertical lines become parabolic under vertical compression, the analytical solution for the effective compression modulus has been derived for bonded rectangular layers. In particular, the QR-transformation permits a closed form solution. The governing equations are then solved by the double series approach, taking advantage of symmetry about the x_1 and x_2 axes. The solution as given by Eq. (36) does not require any mathematical function and is an algebraic function of three parameters, namely Poisson's ratio, the shape factor and the aspect ratio. This

approach provides a direct means for computation of the effective compression modulus. It is much easier to implement than numerical methods such as the finite element method, particularly for parametric study.

The solutions for square layer and infinite strip are special cases of the present solution with the aspect ratio equal to, respectively, unity and an extreme value. Virtually identical results are obtained by the present method as compared to published results for the entire range of Poisson's ratio. For a rectangular layer of 2:1 aspect ratio, the present solution is in good agreement with the finite element solution. Consistent with previous findings, the results show that the assumption of strict incompressibility ($\nu = 0.5$) over-estimates E_c considerably when Poisson's ratio is in fact not 0.5, though close enough.

Parametric studies show that, for given values of shape factor and Poisson's ratio, E_c decreases with the extent of "elongation" (deviation of length from width). The effect of aspect ratio on E_c is more pronounced as Poisson's ratio is near 0.5, and the reduction can be as much as about 40%. The series solution exhibits second-order convergence in both m and n indices. It may therefore be necessary to use more than just the first term; terms up to $m = n = 2$ are recommended for practical use.

References

Chalhoub, M.S., Kelly, J.M., 1990. Effect of bulk compressibility on the stiffness of cylindrical isolation bearings. International Journal of Solids and Structures 26, 734–760.

Chalhoub, M.S., Kelly, J.M., 1991. Analysis of finite-strip-shaped base isolator with elastomer bulk compressibility. Journal of Engineering Mechanics ASCE 117, 1791–1805.

Constantinou, M.C., Kartoum, A., Kelly, J.M., 1992. Analysis of compression of hollow circular elastomeric bearings. Engineering Structures 14, 103–111.

Gent, A.N., Lindley, P.B. 1959. The compression of bonded rubber blocks. Proceedings of Institution of Mechanical Engineers, vol. 173, pp. 111–117.

Gent, A.N., Meinecke, E.A., 1970. Compression, bending, and shear of bonded rubber blocks. Polymer Engineering and Science 10, 48–53.

Kelly, J.M., 1997. Earthquake-resistant design with rubber, 2nd edn. Springer, London.

Koh, C.G., Kelly, J.M., 1989. Compression stiffness of bonded square layers of nearly incompressible material. Engineering Structures 11, 9–15.

Lindley, P.B., 1966. Load-compression relationships of rubber units. Journal of Strain Analysis 1, 190–195.

Lindley, P.B., 1979. Compression moduli for blocks of soft elastic material bonded to rigid end plates. Journal of Strain Analysis 14, 11–16.

Moghe, S.R., Neff, H.F., 1971. Elastic deformations of constrained cylinders. Journal of Applied Mechanics ASME 38, 393–399.

SAP2000, 1997. Structural Analysis Program. Computers and Structures, Berkeley, CA.

Tsai, H.-C., Lee, C.-C., 1998. Compression stiffness of elastic layers bonded between rigid plates. International Journal of Solids and Structures 35, 3053–3069.